J Mater Sci: Mater Med (2012) 23:3003–3014
DOI 10.1007/s10856-012-4742-z

# "In vitro" behaviour of adult mesenchymal stem cells of human bone marrow origin seeded on a novel bioactive ceramics in the $Ca_2SiO_4$–$Ca_3(PO_4)_2$ system

**Luis Meseguer-Olmo · Salvador Aznar-Cervantes · Patricia Mazón · Piedad N. De Aza**

Received: 11 May 2012 / Accepted: 2 August 2012 / Published online: 19 August 2012


**Abstract** This work describes the evaluation of three ceramic materials as potential osteogenic substrate for bone tissue engineering. The capacity of adult human mesenchymal stem cells cultured under experimental conditions known to adhere, proliferate and differentiate into osteoblasts was studied. Two types of culture medium: growth medium and osteogenic medium were evaluated. The materials were pure α-tricalcium phosphate and also αTCP doped with either 1.5 or 3 wt% of dicalcium silicate. The results showed that the *h*MSCs cultured adhered, spread, proliferated and produced mineralized extracellular matrix on all the ceramics studied. They showed an osteoblastic phenotype, especially in the αTCP doped with 1.5 wt% $C_2S$, indicating osteoblastic differentiation as a result of the increased concentration of silicon in solid solution in TCP. Ceramics evaluated in this work are bioactive, cytocompatible and capable of promoting the differentiation of *h*MSCs into osteoblast.

L. Meseguer-Olmo
Service of Orthopaedic Surgery-Bone Bioengineering Unit, University Hospital V.Arrixaca, University of Murcia, 30520 Murcia, Spain
e-mail: lmeseguer.doc@gmail.com

S. Aznar-Cervantes
Department of Biotechnology, IMIDA, La Alberca, 30150 Murcia, Spain
e-mail: sdac1@um.es

P. Mazón
Departamento de Ciencia de Materiales, Óptica y Tecnología Electrónica, Universidad Miguel Hernández, Avda. Universidad s/n, 03202 Elche, Alicante, Spain
e-mail: pmazon@umh.es

P. N. De Aza (✉)
Instituto de Bioingeniería, Universidad Miguel Hernández, Avda. Universidad s/n, 03202 Elche, Alicante, Spain
e-mail: piedad@umh.es

## 1 Introduction

Calcium phosphates (CaP) with clinical applications are used in reconstructive surgery. When dealing with the repairing of a skeletal section, two extremely diverse routes could be initially considered: to replace the damaged part or to substitute it regenerating the bone. This second option is in fact the role played by CaP, which can be classified among the bioactive ceramics group. Bioceramics, and therefore, CaP, exhibit very good biocompatibility and bone integration qualities, and constitute the materials showing closest similarity to the mineral component of bone; this fact, together with their bioactivity, make them very good candidates for bone regeneration.

A lot of interest has been generated in silicon (Si) since the studies of Carlisle [1–3] showed that "Si may be allied to the initiation of mineralization of preosseous tissues". Silicon is essential for the growth and development of certain biological tissues, such as bone, teeth and some invertebrate skeletons. A recent investigation showed that dietary Si intake is positively associated with cortical mineral density subject to availability of estrogens in humans [4]. On the other hand, several authors [5, 6], have not been able to fully reproduce the work reported by Carlisle [1–3] although various moderate effects on bone metabolism have been observed. The exact mechanisms of action of Si on bone are still unclear, and both a structural and metabolic role has been proposed [7–10].

As a consequence, Si-substituted silicon-doped CaP have attracted the interest of many scientists because Si incorporation is considered to be a promising way to

improve the bioactivity of CaP-based biomaterials. [11–15]. These materials exhibited excellent ability to assist in bone-like carbonated hydroxyapatite (CHA) formation "in vitro" and "in vivo". Furthermore, the Si-containing ionic products from bioactive glass possessed the capacity to activate bone-related gene expression as well as to stimulate osteoblast proliferation and differentiation [16, 17]. Therefore, the silicon-containing bioactive materials may open up new possibilities in the field of medical application.

Nowadays, tricalcium phosphate (TCP) is one of the most important calcium phosphate based biomaterials for clinical use because of its biocompatibility, in vivo bioactivity, bioresorbability and osteoconductivity. There are three polymorphs of TCP [18–20] the low temperature, $\beta$-TCP, and the two high temperature forms, $\alpha$-and $\alpha'$-TCP. The last one lacks of practical interest because it only exists at temperatures above $\sim$1,465 $\pm$ 5 °C and reverts to $\alpha$-TCP by cooling below the transition temperature. However, $\beta$-TCP is stable at room temperature and transforms reconstructively at $\sim$1,115 $\pm$ 10 °C to $\alpha$-TCP, which can be retained during cooling to room temperature. Some authors suggest that small amounts of Si in TCP lowers the temperature of phase transition from $\beta$-TCP to $\alpha$-TCP stabilize the phase $\alpha$-TCP at room temperature [11, 14].

To take advantage of the beneficial effect of Si, novel materials with compositions derived from the Dicalcium Silicate—Tricalcium Phosphate phase diagram ($C_2S$–TCP) were developed [21–23] in this study for biomedical application, as Si can be released from the ceramics in situ under "in vitro" conditions. The effect of the $\alpha$TCP solid solution (TCPss) phase composition in terms of $C_2S$ content, which introduced Si element into the structure of the ceramics, on the "in vitro" adult mesenchymal stem cells of human origin (*h*MSCs) attachment, proliferation, and differentiation was therefore investigated.

## 2 Materials and methods

### 2.1 Materials and characterization

The starting materials for the present study were TCP and $C_2S$ previously synthesized [23]. Tricalcium phosphate was synthesized by solid state reaction from a stoichiometric mixture of calcium hydrogen phosphate anhydrous ($CaHPO_4$, Panreac), and calcium carbonate ($CaCO_3$, Fluka) with an average particle size of <15 μm. The mixture of $CaHPO_4$ and $CaCO_3$ was heated in a platinum crucible at 1,500 °C for 3 h. Then was liquid-nitrogen quenched by rapid removal from the furnace. The obtained material was ground and characterized by X-ray diffraction (XRD).

Dicalcium silicate was obtained by solid state reaction-sintering, starting from an appropriate mixture of calcium carbonate, ($CaCO_3$ >99.0 wt% Fluka) with an average particle size of <15 μm, and Si oxide ($SiO_2$ >99.7 wt%, Strem Chemicals), with an average particle size <50 μm. As a preliminary step, $SiO_2$ was wet ground in a laboratory mixing miller (MM301-Retsch) by using PSZ-zirconia balls and isopropyl alcohol as suspension media. The powder was then dried and sieved to <50 μm. The average particle size of the final $SiO_2$ used was 40 μm as measured by laser diffraction (Mastersizer2000E device-Malvern). Next, the desired proportions of the constituents were weighed out and thoroughly wet mixed in a mixing miller with the same $ZrO_2$ balls mentioned above as a grinding media. After the milling process, the mixture was dried and burned at 1,000 °C for 24 h to remove the $CO_2$. Then, this powder was cold isostatically pressed at 200 MPa and heat treated at 1,525 °C for 12 h, at a heating rate of 8.3 °C/min followed by cooling rate of 5 °C/min. The reaction-sintering temperature was selected bearing in mind the information provided by the $SiO_2$–CaO phase equilibria diagram evaluated and reported by Eriksson et al. [24]. The obtained material was ground and characterized by XRD.

$\alpha$TCP ceramic and $\alpha$TCP compositions doped with 1.5 and 3.0 wt% of $C_2S$ (TCPss) were prepared in this study. The desired proportions of each component were weighed out in an analytical balance, dispersed in acetone, and thoroughly mixed in a manual agate mortar. The mixture was isostatically pressed into bars at 200 MPa and the bars were heated up to 1,500 °C for 2 h followed by liquid-nitrogen quenching after rapid removal from the furnace. In order to homogenize the compositions, the bars were ground, pressed and reheated again. This procedure was repeated three times. The final powders with an average particle size of 23 μm were pressed into bars at 200 MPa. The next step involved heating the bars up to 1,500 °C for 4 h, followed by cooling inside the furnace to 1,120 °C, where the bars remained for 16 h before cooling down to room temperature. The heat treatment temperatures were carefully selected bearing in mind the information provided by the $\alpha TCP_{ss}$-Silicocarnotite sub-system from within the binary system of TCP–$C_2S$ [$Ca_3(PO_4)_2$–$Ca_2SiO_4$] [23]. The final samples were cut from the bars obtained, which measured 7 mm in diameter and 1.5 mm in thickness.

To evaluate the phase's composition, XRD patterns were obtained in a Bruker-AXS D8Advance automated diffractometer using CuK$\alpha$1,2 radiation (1.54056 Å) and a secondary curved graphite monochromator. Data were collected in the Bragg–Brentano ($\theta/2\theta$) vertical geometry (flat reflection mode) between 10° and 40° ($2\theta$) at 0.05° steps, counting 6 s per step. Samples were rotated at 30 rpm during acquisition of patterns in order to improve averaging. The diffractometer optic was a system of primary Soller foils between the X-ray tube and the fixed aperture slit. One scattered radiation slit of 1 mm was

placed after the sample, followed by a system of secondary Soller slits and a detector slit of 0.1 mm. The X-ray tube was operated at 40 kV at 30 mA. Diffractograms of samples were compared with the data provided by the Joint Committee on Powder Diffraction Standards (JCPDS) database.

For the microstructural examination, the samples were embedded in an epoxy resin under vacuum and progressively polished to final surface finish of 0.1 μm size using diamond paste, followed by gentle cleaning and etching with acetic acid (1.0 %v/v) for 6 s. Palladium coating was applied to the specimens for observations on SEM-Hitachi S-3500 N. The chemical composition of the specimens was determined with a wavelength dispersive X-ray spectrometer (WDS), coupled to the electron microscope.

## 2.2 Preparation and culture of adult *h*MSCs

### *2.2.1 Isolation and culture of hMSCs*

For testing biocompatibility, adhesion and induction of the proliferation and osteogenic differentiation, adult *h*MSCs (provided by Dr. L. Meseguer-Olmo) were isolated from bone marrow (20–25 ml volumes) obtained by percutaneous direct aspiration from iliac crest of four hematologic healthy volunteers (three men, one women), ranging from 27 to 35 years old (mean = 30.2 years), who underwent elective surgery for slipped disc and a vascular necrosis of the femoral head as a result of traumatic hip dislocation. The volunteers signed previously a consent form. The study was approved by the institutional ethics and clinical trials committee of the University Hospital V. Arrixaca (Murcia, Spain).

For the isolation, whole bone marrow aspirated was suspended in a tube containing sodium heparin (20 U $ml^{-1}$ of aspirated material). Mononuclear cell were obtained from buffy coat by ficoll gradient through an automated device closed SEPAX$^{TM}$ System (Biosafe, Eysines, Switzerland), then the count was performed with a Neubauer chamber.

After estimating the viability with vital staining (Trypan blue), the mononuclear cells were plated at $5.0 \times 10^3$ cells/$cm^2$ in 75 $cm^2$ culture flasks (Sarsted) with 10 ml of basal growth medium (GM) and they were incubated at 37 °C, in a 5 % $CO_2$ and 95 % of relative humidity atmosphere and remained, to attach, undisturbed for 7 days. The basal GM consisting of α-modified Eagle′s medium (αMEM) supplemented with 10 % heat inactivated fetal bovine serum (FBS) and penicillin/streptomycin 100 U $ml^{-1}$ and 100 μg $ml^{-1}$, respectively.

### *2.2.2 Subcultures of hMSCs*

After 7 days, the culture medium was renewed removing thus the non-adherent hematopoietic cells and selecting the *h*MSCs given their proved capacity of attaching to the plastic of culture flasks [25]. When cells reached 80–90 % confluence, they were subcultured in a 1:3 ratio treating the culture flask with trypsin/EDTA (0.25/0.25 %) in phosphate-buffered saline (PBS, pH 7.4) for 5 min. To obtain the homogeneity of the sample and reduce inter-individual variability among donors, and the amount of donors needed, all the cells from the first subculture (passage 1, P1) were pooled and replated in 175 $cm^2$ flasks ($5.0 \times 10^3$ cells/$cm^2$) for growing and to obtain a sufficient number of cells until use in the study in passage 3 (P3). The culture medium was changed twice every week.

### *2.2.3 Cell characterization*

In order to confirm the identity of isolated cells, the adherent isolated cells, considered as *h*MSCs, were tested for the expression of the membrane antigen markers [cluster of differentiation (CD)] CD73, CD90 and CD105 markers and the negative expression markers CD34 and CD45 hematopoietic markers using specific mouse anti-human monoclonal antibodies (CD34-PE, CD45-FITC, CD73-PE, CD90-APC, CD105-FITC). Isotype controls for each fluorochrome (FITC, PE and APC) were anti-mouse immunoglobulin (IgG1, k) (all from BD Biosciences. San Diego, CA, USA). Samples were acquired by a flow cytometer from Beckman Coulter Navios Ships type and analyzed with FCS Express V3 program (data not included). After that, the cells were identified as undifferentiated *h*MSCs.

## 2.3 Behaviour of *h*MSCs on the ceramics and characterization

For the study of the biocompatibility and behaviour of isolated *h*MSCs on ceramics, two culture media were used:

(1) Growth medium (GM). This medium was used for cell isolation and expansion. It consists of αMEM supplemented with 10 % of heat-inactivated FBS and penicillin/streptomycin (100 U $ml^{-1}$ and 100 μg $ml^{-1}$, respectively).
(2) Osteogenic medium (OM; differentiation medium). This medium consists of GM with an osteogenic supplement (OS) composed of L-ascorbic acid-2-phosphate (0.2 mM; Sigma), dexamethasone (10 nM; Sigma) and β-glycerolphosphate (10 mM; Merck).

Initially, the ceramic discs were cleaned with pressured air, rinsed several times with PBS (pH 7.4), dried at 37 °C and sterilized at low temperature by gas plasma (Sterrad-100S$^{TM}$, ASP Irvine, Ca). Discs were pre-wetted in GM for 2 h prior seeding. Then, they were placed inside the wells of a 96-well culture plate. One series of 96-well plates was

seeded in GM and another one was seeded in OM. A total of $1.0 \times 10^4$ cells were statically seeded onto each disc for all assays. The incubation was carried out in standard conditions mentioned before (37 °C, 5 % $CO_2$ and 95 % humidity). Cell biocompatibility and behaviour were analysed at 24 h and 7, 15, 21 and 28 days by means of a proliferation assay, scanning electron microscopy (SEM) and osteoblastic phenotype expression.

#### 2.3.1 Proliferation assay

The increment in the cells' number on materials surfaces using both media (GM and OM) was quantified spectrophotometrically through with a tetrazolium salts assay (XTT), using the method described by Scudiero et al. [26]. Briefly, XTT with PMS was added to each well and after 4 h of incubation, absorbance of the culture medium of the cells growing on the ceramic pellets was measured at 450 nm in a plate reader Multiskan MCC 340 (Labsystem, CO, USA). Another series of *h*MSCs were seeded onto plastic in order to be used as a quality control of the cells seeded onto the bioceramics. The proliferation of *h*MSCs was analysed at 24 h and at days 7, 15, 21 and 28 days. The results are reported as optical density (OD) values. All assays were performed in triplicate ($n = 3$).

#### 2.3.2 Morphological evaluation. Scanning electron microscopy

Before cell culture studies, and in order to recognize the surface of the ceramic seeded, one of the faces of the samples was carefully impressed with an electrical marked. Qualitative analysis of *h*MSCs morphology along the materials surface was performed at 24 h, and 7, 21, and 28 days of culture. Samples were prepared according to previously reported SEM protocols [15]. Briefly, samples removed from the culture wells were rinsed with PBS and fixed with 3 % glutaraldehyde in 0.1 M cacodylate buffer for 1.5 h at 4° C. Then they were again rinsed and post-fixed in osmium tetroxide for 1 h, before being dehydrated in a series of graded ethanol solutions (30, 50, 70, 90 vol%). Final drying was performed by a critical-point method (CPDO2 Balzers Union) and then sputter coated with gold. Gold coated specimens were examined in the SEM operating at 15 kV, while for WDS analysis the samples were palladium coated.

#### 2.3.3 Osteoblastic phenotype expression

Seeded materials and cultured in both media were assayed, qualitatively or quantitatively, for the presence of osteoblast differentiation markers. Osteocalcine production is a biochemical marker characteristic exclusively of osteoblasts. For that reason, it was used in this work, together with alkaline phosphatase activity, collagen type I expression and mineralization, in order to evaluate if any differentiating effect of *h*MSCs cell into osteoblasts (OBs) had taken place by effect of the materials in both culture conditions (GM and OM). So, the ability of *h*MSCs to differentiate into OBs was studied by determining the production of: ALP (alkaline phosphatase detection kit, Millipore), collagen type I (Col-I immunohistochemical staining. Millipore), osteocalcin (Gla-type osteocalcin EIA kit, Reactive) and nodules of mineralization (osteogenesis Quantitation kit, Millipore), following the manufacturer's instructions. All determinations were performed in triplicate.

### 2.4 Si, Ca and P analyses in culture media

Changes in the ionic concentrations of the culture media were also recorded at 12, 24 h, 3 days, 1 and 2 week periods. After media collection solutions (three samples per period) were stored at 4 °C until analysis. The changes in ionic concentration were measured using inductively plasma optical emission spectroscopy (ICP-OES, Perkin-Elmer Optima 2000$^{TM}$).

### 2.5 Statistical analysis

A repeated measures analysis of variance (ANOVA) was carried out with a level of statistical significance of $P < 0.05$. This was possible because, after applying a natural logarithm transformation to the data, they fulfilled the conditions of homoscedasticity and sphericity required for the analysis.

## 3 Results

### 3.1 Characterization of the ceramics

Figure 1 shows the XRD patterns of the synthesized powder of TCP and $C_2S$ as well as the 1.5 and 3.0 wt% $C_2S$ compositions. It can be seen that the polymorphic form obtained is α-TCP corresponding to JCPDS Card No. 9-348. On the other hand, the $C_2S$ correspond to JCPDS Card No. 87-1257 that belongs to the polymorphic form γ-$C_2S$. The peaks' intensities depended on the $C_2S$ content in αTCP. A review of the X-ray powder diffraction spectra of pure calcium phosphate and silica-doped calcium phosphate, presented by the JCPDS, suggested that only a significant amount of a crystalline phase can give rise to the diffraction pattern. A progressive shift of the main peaks occurred in the XRD spectra obtained for the $C_2S$-αTCP compounds in this study, as the Si content increased. For αTCP, the position of the peak was at 30.8 ($2\theta$) degrees,

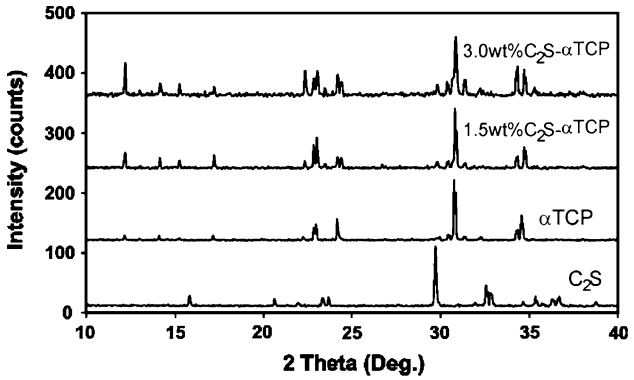


**Fig. 1** XRD patterns of the synthesized powder of αTCP and $C_2S$ as well as the 1.5 wt% $C_2S$-αTCP and 3.0 wt% $C_2S$-αTCP compositions

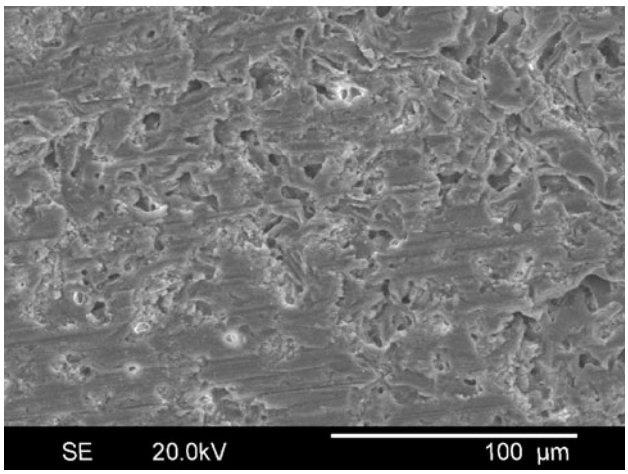


**Fig. 2** SEM micrograph of the unpolished 3.0 wt% $C_2S$-αTCP ceramic surface

while for the 1.5 wt% $C_2S$-αTCP and 3.0 wt% $C_2S$-αTCP compositions, the peak position occurred at 31.0 ($2\theta$) degrees and 31.2 ($2\theta$) degrees respectively, which is in accordance with the JCPDS card 00-058-0897 for the Si-TCP compound. It was also found that the peaks at about 35 ($2\theta$) degrees appeared separated for the 1.5 wt% $C_2S$-αTCP and 3.0 wt%-α$C_2S$ compositions, because of the the Si presence in their structure. Intensities of the other peaks at 12.09 ($2\theta$) and 24.10 ($2\theta$) degrees, which are solely characteristic of the αTCP composition increased significantly with an increase in the $C_2S$ content in the solid solution of αTCP. These results confirmed that the 1.5 wt% $C_2S$-αTCP and 3.0 wt% $C_2S$-αTCP ceramics were composed of a single phase of the solid solution of $C_2S$ in αTCP (named in this study αTCPss).

Based on XRD patterns, the grain size decreased with the increasing Si content from 207 nm for the pure α-TCP to 194 and 129 nm for 1.5 and 3.0 wt% $C_2S$ respectively. This finding agreed with the data reported in the literature for Si doped ceramics, prepared by other chemical methods [14, 27].

The bioceramic surfaces of the as manufactured specimens showed a rough topography, as observed in the SEM prior to the "in vitro" and "in vivo" studies. Figure 2 displays a SEM micrograph of the 3.0 wt% $C_2S$-αTCP ceramic, as representative of all the compositions. Open surface pores progressing into the material were very characteristic with the grain structure clearly visible within the larger pores.

### 3.2 Behaviour of the *h*MSCs on TCPss

Figures 3 and 4 shows the morphology of *h*MSCs adhering and spreading on the all tested ceramic surfaces after culturing for 24 h, 7, 21 and 28 days in GM y OM. When compared with the original surface, before exposure to cell culture medium (Fig. 2), it became evident that the surface morphology was altered for both media.

In the first 24 h of culture in GM (Fig. 3a) the ceramics exhibited a granular layer covering some parts of the surface which is not an obstacle for cell adhesion or proliferation. This layer was composed of uniform ~1 µm size, globular structures with spicules and small nodules which were both composed of Ca–P elements, according to the WDS elemental microanalysis. Later (7 days), the *h*MSCs growing on the ceramic surfaces (Fig. 3b) showed some cells adhering either individually or in small groups dispersed across the granular surface of the material. At this point, *h*MSCs displayed a flattened shape. The adhesion was enhanced by means of multiple cytoplasmic filopodia that spread across the surface of the material, increasing the contact area with the surface material.

After the 21 days exposure period, a fast and progressive growth of the cells was observed on the surfaces (Fig. 3c). The cells formed a monolayer covering partially the material surfaces, and also produced a dense extracellular matrix (ExM) by way of a fibrillar network occupying the intercellular gaps. Some mineralized nodules were also found on the cells' surfaces.

After the period of 28 days (Fig. 3d), the *h*MSCs cells began to organize into a monolayer on all tested materials but in a slightly different manner. On the 1.5 % $C_2S$-αTCP and 3.0 % $C_2S$-αTCP surfaces, the cell monolayer appeared almost continuous with the cells presenting a flattened and spread morphology. On the Si free αTCP surface, the cell to cell contacts were frequent, with numerous intercellular gaps present. In the interaction regions, numerous short filopodia anchored onto the peaks protruding from the surface were clearly observed.

When culture condition were in OM, the behaviour of the cells at 24 h (Fig. 4a) were very similar than in GM (Fig. 3a) due to the formation of a calcium phosphate globular deposit on the surface and inside the pores of each

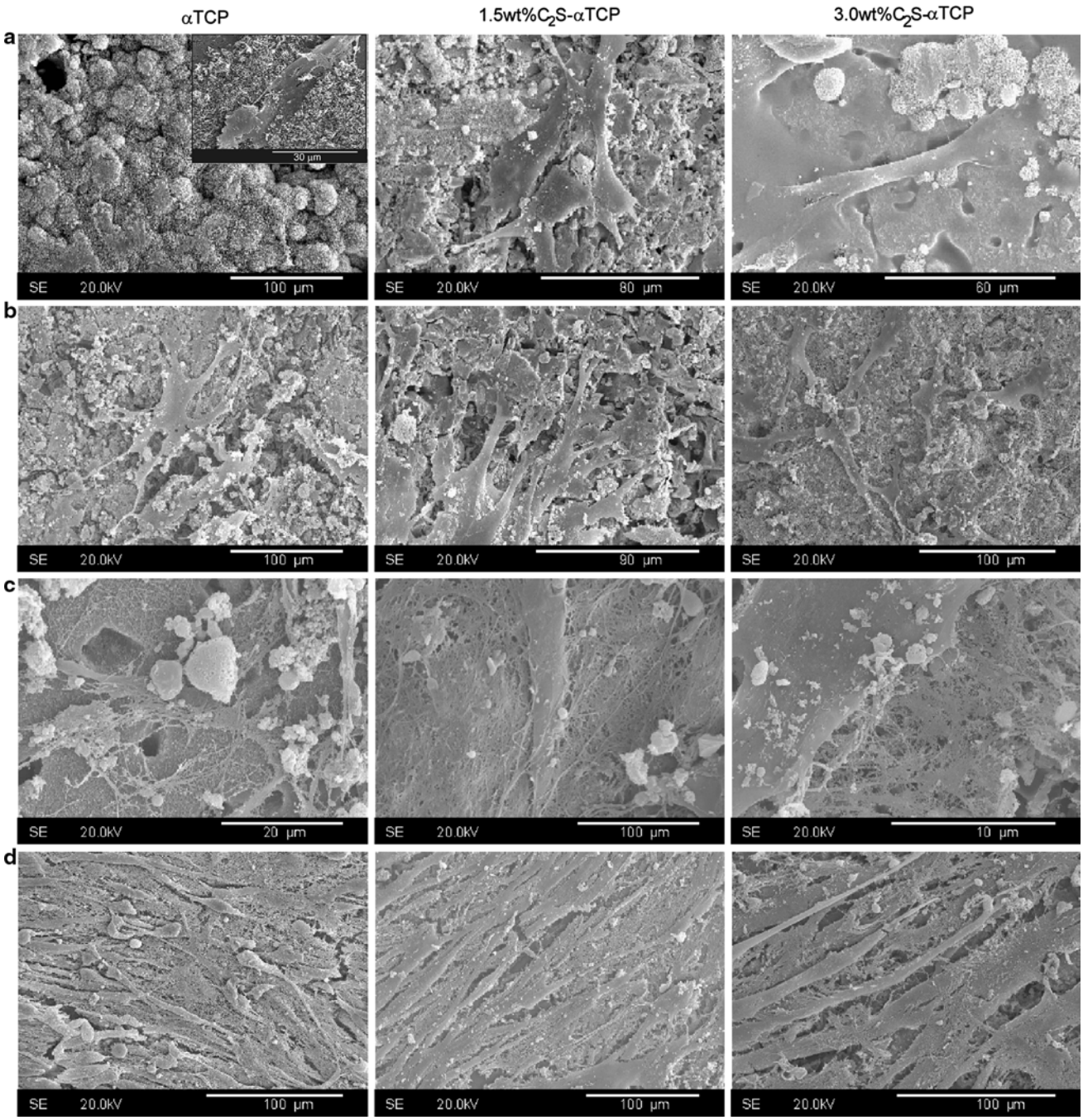


**Fig. 3** SEM images of the *h*MSCs stem cells growing on the ceramics' surfaces after **a** 24 h, **b** 7, **c** 21 and **d** 28 days in GM

ceramic that according to WDS microanalysis indicated mainly Ca and P elements. After 7 days, (Fig. 4b), the cells shows a flattened appearance with spreading cytoplasmatic extensions (filopodia) and presented a close contact with the material. Figure 4c shows a good cell development and proliferation on every ceramic after 21 days of culture. It is also possible to see several mineralization nodules on the cells and in their surroundings. Cells increased in number and formed aggregates, partially coating the surface of the ceramics. After 28 days (Fig. 4d), cell proliferation continued on every ceramic, but the original ceramic could also be seen between the cells and noticeable amounts of calcium phosphate deposits on the ExM was present.

### *3.2.1 Proliferation assay*

The XTT cell proliferation assay confirmed the SEM observations, showing faster and better *h*MSCs cells'

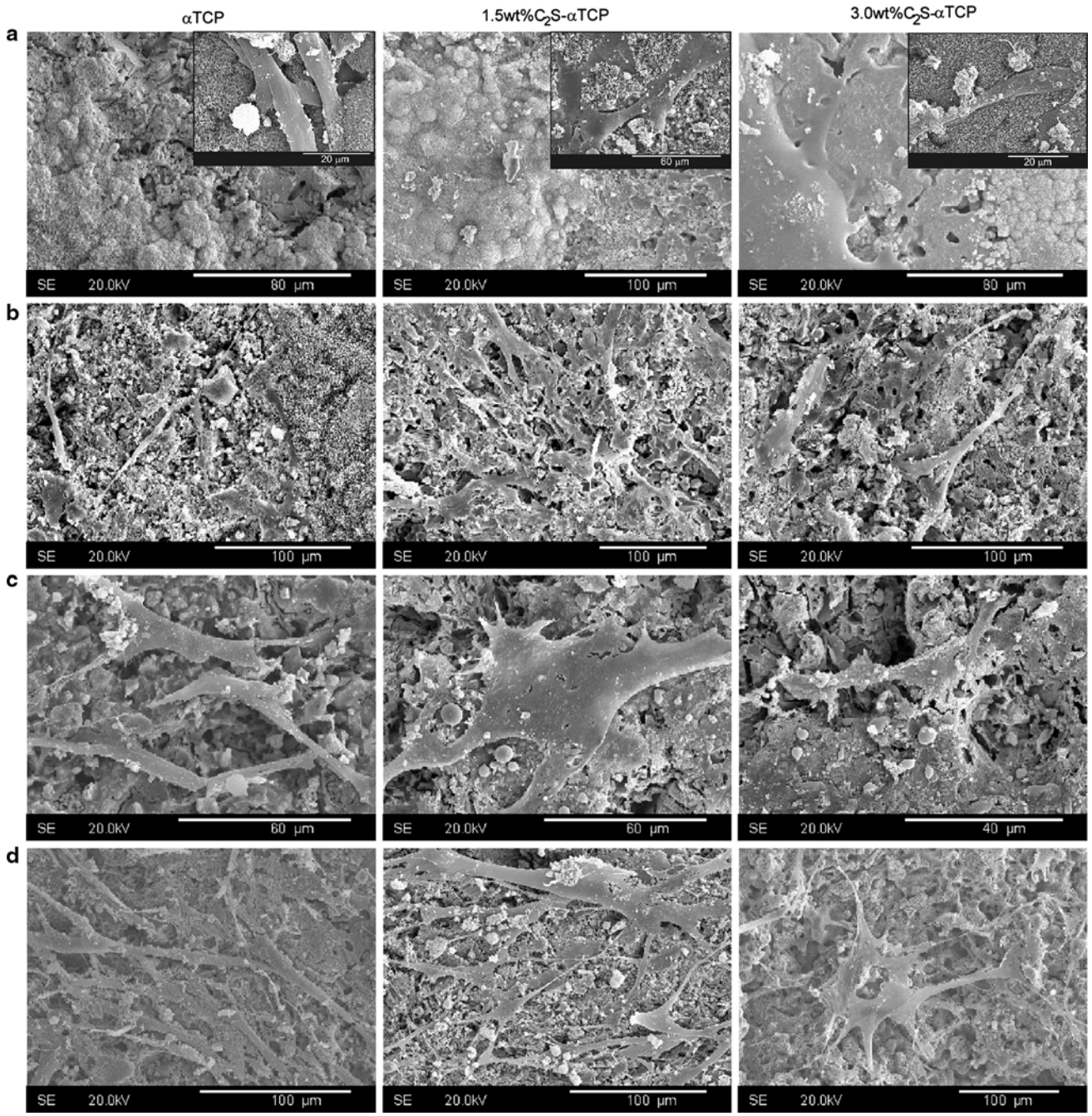


**Fig. 4** SEM images of the *h*MSCs stem cells growing on the ceramics' surfaces after **a** 24 h, **b** 7, **c** 21 and **d** 28 days in OM

proliferation on the 1.5 wt% $C_2S$-αTCP material right from the start of the culture study, than in case of the other two materials ($P < 0.05$). Figure 5 shows the proliferation of the cells on the surfaces of the specimens over the culture time on GM. After 15 days of the culture, there was a clear exponential increase in the absorbance results for the 1.5 wt% $C_2S$-αTCP sample. At the end of the experiment, after 28 days of the culture, the number of cells growing onto the 1.5 wt% $C_2S$-αTCP material was twice as much as in case of αTCP. The proliferation of the cells on the 3 wt% $C_2S$-αTCP material remained almost constant over the whole culture time.

Respect to the *h*MSCs cultured in OM and in contrast with the results above described, cells cultured in OM didn't increase their absorbance values over time, indicating the absence of cell proliferation in this medium with any of the ceramics assayed. Only at the end of the study it could be detected a slight increase in cell number of *h*MSCs growing in 3.0 wt% $C_2S$ and 1.5 wt% $C_2S$-αTCP ceramics.

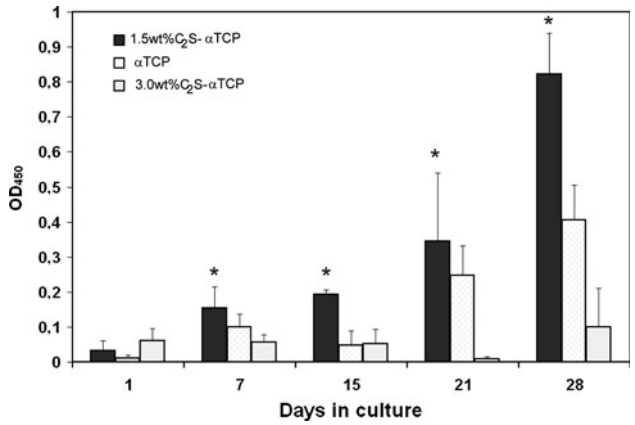


**Fig. 5** XTT assay. *h*MSCs proliferation on materials under study. Results at different times of study. Values obtained for the material 1.5 wt% $C_2S$ are significant ($P < 0.05$) compared to the other two materials studied

### 3.2.2 *Osteoblastic phenotype expression*

*h*MSCs cultured on any of the materials studied produced detectable amounts of osteocalcin, nodules of mineralization, alkaline phosphatase activity and collagen type I expression, independently of the culture medium employed, confirming the differentiation of these cells into OBs by means of the expression of the most characteristic features of this cell type. Histochemical ALP staining, Alizarin Red staining and collagen type I of 1.5 wt% $C_2S$-αTCP ceramic as a representative of all the ceramics is shown in Fig. 6.

*h*MSCs growing in OM showed a stronger stain for collagen-I and alkaline phosphatase as well as more mineralization nodules at the end of the study respect to the cells growing in GM, in spite of the smaller number of cell detected by XTT assay. Only in the case of the osteocalcine (Fig. 7) the expression was higher in GM, probably due to the higher final number of cells in this medium, that in this case influence the results because of this assay is a quantitative assay.

### 3.2.3 *ExM synthesis*

At 14 days, the *h*MSCs cultured in both culture media were able to produce ExM, which formed a fibrillar network occupying the intercellular gaps. This was more evident in cultures with GM, where deposits of granular material with a whitish appearance were also identified within the fibrillar network (Figs. 3c, 4c).

On the other hand, the ExM developed on the discs apparently had identical morphological characteristics. To determine the nature of these nodules, microanalysis by SEM-WDS was carried out. This analysis proved that it was a calcium phosphate based material and therefore

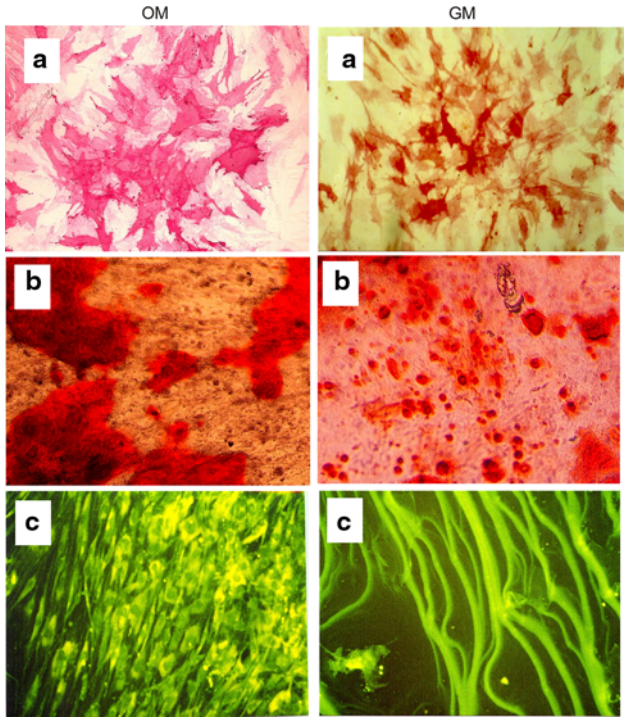


**Fig. 6** Histochemical ALP staining, Alizarin *Red* staining and collagen-I images of *h*MSCs growing in GM and OM media on 1.5 wt% $C_2S$ ceramic as a representative of all the ceramics **a** *h*MSCs were positive for alkaline phosphatase staining, acquiring a *reddish* tint (×120 magnification), **b** Mineral deposits are stained *bright red* by the Alizarin *Red* solution (×120 magnification) and **c** collagen-I (×125 magnification) (Color figure online)

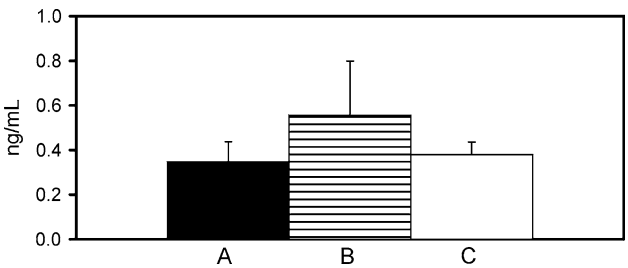


**Fig. 7** Osteocalcine production by *h*MSCs in GM after 28 days of growing on the **a** αTCP, **b** 1.5 wt% $C_2S$-αTCP and **c** 3.0 wt% $C_2S$-αTCP ceramic disks surface

showed a spectrum mainly composed of P and Ca, similar to the one observed in the cytoplasmatic membrane nodules previously described (Figs. 3c, 4c). It is worth noting that these WDS spectra are different to that of the TCPss surface, which showed a big peak corresponding to Si, in addition to Ca and P.

## 3.3 Si, Ca and P analyses in culture media

The effect of culture medium on dissolution rates and release of soluble Si, Ca, P are shown in Table 1. A faster

**Table 1** ICP-OES assay. Concentrations of $Si^{4+}$, $Ca^{++}$, $HPO_4^{=}$ in GM and OM over different immersion times, [n.d. = not detected]

| | | GM | | | OM | | |
|---|---|---|---|---|---|---|---|
| ppm | | Ca | P | Si | Ca | P | Si |
| αTCP | 12 h | 240.97 | 127.30 | n.d | 244.50 | 37.36 | n.d |
| | 24 h | 229.28 | 123.37 | n.d | 241.80 | 314.02 | n.d |
| | 3 days | 236.77 | 121.48 | n.d | 238.20 | 269.30 | n.d |
| | 1 week | 257.00 | 127.01 | n.d | 240.90 | 270.03 | n.d |
| | 2 weeks | 241.50 | 127.34 | n.d | 244.80 | 273.01 | n.d |
| 1.5 wt% $C_2S$-αTCP | 12 h | 256.40 | 129.81 | 0.95 | 263.80 | 278.00 | 1.73 |
| | 24 h | 285.50 | 122.95 | 1.20 | 260.00 | 255.01 | 1.96 |
| | 3 days | 318.81 | 133.42 | 1.93 | 262.00 | 227.06 | 2.16 |
| | 1 week | 320.00 | 128.87 | 2.41 | 256.60 | 209.00 | 2.91 |
| | 2 weeks | 314.00 | 129.06 | 2.42 | 260.50 | 209.02 | 3.06 |
| 3.0 wt% $C_2S$-αTCP | 12 h | 188.00 | 134.08 | 2.20 | 200.80 | 303.00 | 2.64 |
| | 24 h | 197.00 | 127.29 | 2.44 | 208.80 | 270.00 | 3.03 |
| | 3 days | 212.00 | 141.43 | 2.95 | 215.70 | 246.00 | 3.26 |
| | 1 week | 236.84 | 140.87 | 4.62 | 228.20 | 236.00 | 5.15 |
| | 2 weeks | 230.96 | 141.10 | 4.74 | 224.00 | 224.00 | 5.20 |

dissolution rate with respect to Si was seen for 3.0 wt% $C_2S$-αTCP compared to 1.5 wt% $C_2S$-αTCP, which we ascribed to the greater specific surface area of the finer-grain size (129–194 nm respectively).

Growth and osteogenic media appeared to have similar effects in terms of faster dissolution rate of the TCPss ceramics and Si levels (Table 1-OM-Si vs. Table 1-GM-Si). Some differences were evident, however, in Ca and P concentration profiles between GM and OM media. Calcium concentrations reached steady state earlier (1.5 wt% $C_2S$-αTCP = 3 days; 3.0 wt% $C_2S$-αTCP = 1 week) in GM than in OM where steady state had not been achieved even at 2 weeks (Table 1-OM-Ca vs. Table 1-GM-Ca).

Concentration of the P element changed slightly for the αTCP and 1.5 wt% $C_2S$-αTCP ceramics, meaning that the consumption rate of the P ions due to the precipitation of the Ca–P layer remained the same as the P ion release rate from the ceramics. The lower initial P in GM also limited CaP precipitation so that less Ca is removed from solution. Therefore, final Ca levels were higher for TCPss in GM than in OM.

The initially higher content of Si and lower Ca levels observed in both media for 3.0 wt% $C_2S$-αTCP in comparison to 1.5 wt% $C_2S$-αTCP indicated a faster dissolution rate of the 3.0 wt% $C_2S$-αTCP material, hence faster precipitation rate of the Ca–P on the surface of the ceramic. The 3.0 wt% $C_2S$-αTCP ceramic was composed of the smallest grain size, in comparison with the other two materials, hence presented a faster dissolution rate of Ca, P, Si elements. These differences in the dissolution rates between the ceramics during the immersion in the culture medium could potentially influence the cells' activities.

## 4 Discussion

Surgeons dedicated to reconstructive surgery of bone tissue are often faced with the challenge of repairing large bone defects. The traditional procedures involving the use of autologous cancellous bone tissue, a technique that has major drawbacks (pain in donor site, hematoma, infection, bleeding, hernia, etc.). To avoid such disadvantages the tissue engineering offers new strategies to enhance the utility of biomaterials for the development of new treatment in bone replacement technology. The association of osteogenic precursor cells (*h*MSCs) to biomaterials with the ability to initiate osteoblastic differentiation "in vitro" before implantation can accelerate the bone formation process after being implanted into the bone defect.

The present work study the biological responses of the αTCP ceramic free from Si, and αTCP doped with either 1.5 wt% $C_2S$ or 3.0 wt% $C_2S$ in view of the beneficial effect of the Si element presence in osseointegration of the bone substitute materials and as a pre-osteoblastic inducer, without any addition of other osteogenic inducers commonly used, such as, vit C, dexamethasone, etc. The study used adult mesenchymal stem cells of human origin, which have frequently been used to elucidate the responses of bone cells to biomaterials [28–31].

The TCPss ceramics obtained present a bioactive surface that shows formation of a calcium phosphate layer after exposure for 24 h to OM and GM (Figs. 3a, 4a). This layer will play an essential role in the primary chemical bonding of the material after implantation into the receptor osseous tissue.

Regarding the morphology of the cells growing on the ceramics studied initially showed a spreading habit, with cytoplasmatic digitations and a smooth, homogeneous cell membrane. The cells showed good adhesion to the materials surface according to their spreading. Furthermore, the cells presented abundant filopodia and intercellular connections (Figs. 3b, 4d). The material 1.5 wt% $C_2S$-$\alpha$TCP is the one that present more and better grown and proliferation of cell shows, followed by pure $\alpha$-TCP and 3 wt% $C_2S$-$\alpha$TCP ceramics.

Several studies [32–34] have shown that surface roughness of a bioactive implant is an important factor in basic cell biological responses, improving cells' attachment and proliferation. Other studies found that the *h*MSCs stem cells demonstrate significantly higher levels of the cells' attachment on rough sandblasted surfaces with irregular morphologies than on smooth surfaces [23]. The ceramic samples developed in this study exhibited an uneven surface topography, as shown in Fig. 2, hence the surface properties of the material can help to promote the *h*MSCs cells' attachment.

The capacity of cells to produce mineralized matrix and mineralization nodules is taken into account in the design and development of materials for bone regeneration. The cells growing in the presence of the ceramics were able to produce small mineral deposits showing a WDS spectrum composed of Ca and P both in the ExM core and in the proximities of the cells (Figs. 3b–c, 4c–d) This effect was also observed with other types of bioactive ceramic [35–38].

*h*MSCs cultured on any of the materials studied were able to differentiate to OBs independently of the addition of supplements to the medium like L-ascorbic acid-2-phosphate, dexamethasone and $\beta$-glycerolphosphate (OM). It has been reported that this supplements are necessaries in order to the differentiation into OBs took place. Despite of it was evident a stronger stain for ALP, col-I an mineralization nodules when these supplements were in the culture medium, the differentiation also happened in GM, probably due, to their presence in the foetal bovine serum, though it also could be taken in account a possible effect of the ceramics, which should be demonstrated in a serum free medium. According our results it should be advisable to supplement the culture medium with a osteogenic supplement in order to get a better and stronger differentiation of *h*MSCs into OBs, but not for achieving their proliferation.

At this point it is important to note that the inductive effect of TCPss materials on *h*MSCs differentiation into OBs could be favoured by the Si in solid solution in the TCP ceramics as well as the release of Si and Ca ions into the culture medium and the formation of the previously mentioned Ca–P layer (Figs. 3a, 4a; Table 1) These phenomena agree with previous studies of bioactivity in SBF [39] The TCPss ceramic exposed to SBF releases Ca and Si ions to the medium and finally shows the formation on its surface of a carbohydroxyapatite layer 24.5 % greater than pure $\alpha$TCP. Furthermore, different studies have found similar behaviour of materials in SBF and culture medium [28, 40, 41]. Hence, formation of the CaP layer by release of Ca and Si ions into the culture medium stimulates OBs proliferation.

It is believed that Si ions play an important role in mineralization and nodule formation. An appropriate concentration of Si in the biomaterial acts as a stimulant for bone matrix integration because of the ion exchange mechanism with the surrounding environment [16, 42–46]. However, higher Si concentrations appeared to cause cells' death. Our extensive literature review on soluble factor effects showed that Si concentrations <19 ppm or Ca concentrations ~250–600 ppm favour osteoblastic differentiation and viability [16, 42–46]. There appears, thus, an optimal concentration range for these soluble factors to stimulate the cell's differentiation.

The Si concentrations from the 1.5 wt% $C_2S$-$\alpha$TCP increased from ~0.95 to 2.42 ppm by 2 weeks (Table 1-GM) and 1.73 to 306 ppm by 2 weeks (Table 1-OM), and Ca concentration increased to 314 ppm (Table 1-GM) and 260 ppm (Table 1-OM). The initial Si and Ca concentrations from the 3 wt% $C_2S$-$\alpha$TCP were very different, with much higher initial Si concentration (~2.20 ppm-GM and 2.64 ppm OM) and lower Ca concentration (<250 ppm GM and OM). Subsequent Ca concentration continued to be lower for the 3 wt% $C_2S$-$\alpha$TCP, but P concentration increased compared to the 1.5 wt% $C_2S$-$\alpha$TCP (GM and OM).

The effect of Ca concentrations >250 ppm on promoting the cell viability in presence of the 1.5 wt% $C_2S$-$\alpha$TCP ceramic was matched by the pro-osteogenic effect of the higher P concentration present in media during exposure of the 3 wt% $C_2S$-$\alpha$TCP at the end of the 2 week study. These changes in the soluble factor concentrations may affect the cells' proliferation and OC production, which was lower during the 3.0 wt% $C_2S$-$\alpha$TCP exposure than in case of the 1.5 wt% $C_2S$-$\alpha$TCP. The results showed that an optimal concentration range of the soluble elements may be needed in the media, in order to secure the cells' growth and proliferation during the exposure.

The concept of an optimal concentration range is supported by a previous in vivo study in New Zealand rabbits [47] showing that 1.5 wt% $C_2S$-$\alpha$TCP ceramics supported significantly more bone in-growth than 3 wt% $C_2S$-$\alpha$TCP ceramics. Also, as we concluded for cell growth and proliferation, different soluble factors may have different influences and may act cooperatively or in opposition.

Some authors have been proposed several mechanisms, either active or passive to explain that the addition of Si to CaP modifies the "in vitro" and "in vivo" behaviour of Si-substituted CaP. When active mechanisms are involved, Si ions are released and are ''seen'' by cells, hence affecting their metabolism. It has been documented that bioactive glasses and ceramics exert a genetic control over osteoblastic

cell cycle and a rapid expression of genes that regulate osteogenesis and the production of growth factor [48–50]. Silicon has been identified as the major contributor to the mineralization of bone and gene activation [48–50]. When passive mechanisms are involved, the presence of Si in the CaP structure causes change of grain size [51–53], a change of protein conformation at the material surface [45] or a change of surface topography, since surface topography affects the cellular behaviour [44, 54], and since a decrease of grain size was observed with an increase in Si-substitution degree [14, 46, 47]. The mechanism by which the TCPss evaluated in this work induces the differentiation of *h*MSCs into OBs will be investigated in future works.

The present results verify that features such as composition and roughness can modulate cells responses "in vitro". Both the steady adhesion of cells on the substrate surface and the osteocalcine production are data that should be considered in the evaluation of the material cytocompatibility. In our study, excellent cell adhesion and proliferation were observed, as well as an increase in the osteocalcine production.

## 5 Conclusion

The powder metallurgy method combined with the appropriate homogenisation and heat treatment procedures was successful in obtaining pure αTCP composition and also Si doped compositions containing either 1.5 or 3.0 wt% of $C_2S$ in αTCP ceramics. All materials were composed of a single phase, which was stable at room temperature. $C_2S$ formed a solid solution with αTCP, called in the paper αTCPss.

The αTCPss ceramic evaluated in this work provided a favourable microenvironment for the adhesion, spread and proliferation of *h*MSCs, and it was improved with culture time. The *h*MSCs expressed markers of the osteoblastic phenotype (ALP activity, Col I expression, OC production and mineralization) in the α-TCPss materials indicating osteoblastic differentiation as a result of the increased concentration of Si in solid solution in α-TCP. These findings are consistent with the importance of "in vitro" osteoblastic *h*MSCs pre-orientation for, later, to initiate bone formation in vivo. Respect to the two culture mediums employed, GM should be used for proliferation of *h*MSCs and OM only for differentiation studies or for detecting osteoblastic phenotype.

The TCPss ceramics behaves as a cytocompatible and bioactive materials able to induce "*per se*" osteoblastic differentiation of *h*MSCs which would contribute to the quick bonding of the materials to the receptor bone in vivo. So, TCPss ceramics should be an effective substrate promoter of bone tissue regeneration suitable for bone tissue bioengineering.

**Acknowledgments** Part of this work was supported by CICYT under Project No. MAT2006-12749-C02-02.

## References

1. Carlisle EM. Silicon: a possible factor in bone calcification. Science. 1970;167:279–80.
2. Carlisle EM. Silicon: an essential element for the chick. Science. 1972;178:619–21.
3. Carlisle EM. A silicon requirement for normal skull formation in chicks. J Nutr. 1980;110:352–9.
4. Seaborn CD, Nielsen FH. Dietary silicon and arginine affect mineral element composition of rat femur and vertebra. Biol Trace Elem Res. 2002;89:239–50.
5. Nielsen FH, Poellot R. Dietary silicon affects bone turnover differently in ovariectomised and sham-operated growing rats. J Trace Elem Exp Med. 2004;17:137–49.
6. Jugdaohsingh R, Calomme MR, Robinson K, Nielsene F, Anderson SHC, D'Haese P, Geusens P, Loveridge N, Thompson RPH, Powell JJ. Increased longitudinal growth in rats on a silicon-depleted diet. Bone. 2008;43:596–606.
7. Carlisle EM. Silicon as an essential trace element in animal nutrition. In: Evered D, O'Connor M, editors. Silicon biochemistry, Ciba foundation symposium 121. Chichester: Wiley; 1986. p. 123–39.
8. Reffitt DM, Ogston N, Jugdaohsingh R, Cheung HF, Evans BA, Thompson RP, et al. Orthosilicic acid stimulates collagen type I synthesis and osteoblastic differentiation in human osteoblast-like cells "in vitro". Bone. 2003;32:127–35.
9. Jugdaohsingh R. Silicon and bone health. J Nutr Health Ageing. 2007;11:99–110.
10. Jugdaohsingh R, Tucker KL, Qiao N, Cupples LA, Kiel DP, Powell JJ. Dietary silicon intake is positively associated with bone mineral density in men and premenopausal women of the Framingham Offspring cohort. J Bone Miner Res. 2004;19:297–307.
11. Pietak AM, Sayer M. Functional atomic force microscopy investigation of osteopontin affinity for silicon stabilized tricalcium phosphate bioceramic surfaces. Biomaterials. 2006;27:3–14.
12. Dorozhkin SV. "In vitro" mineralization of silicon containing calcium phosphate bioceramics. J Am Ceram Soc. 2007;90(1):244–9.
13. Minarelli-Gaspar AM, Saska S, Carrodeguas RG, De Aza AH, Pena P, De Aza PN, et al. Biological response to wollastonite doped α-tricalcium phosphate implants in hard and soft tissues in rats. Key Eng Mater. 2009;396–398:7–10.
14. Martinez IM, Velasquez PA, de Aza PN. Synthesis and stability of α-tricalcium phosphate doped with dicalcium silicate in the system $Ca_3(PO_4)_2$–$Ca_2SiO_4$. Mat Charact. 2010;61:761–7.
15. Martinez IM, Velasquez P, Meseguer-Olmo L, De Aza PN. Production and study of "in vitro" behaviour of monolithic α-tricalcium phosphate based ceramics in the system $Ca_3(PO_4)_2$–$Ca_2SiO_4$. Ceram Int. 2011;37:2527–35.
16. Xynos ID, Edgar AJ, Buttery LDK, Hench LL, Polak JM. Ionic products of bioactive glass dissolution increase proliferation of human osteoblasts and induce insulin-like growth factor II mRNA expression and protein synthesis. Biomed Biophys Res Commun. 2000;276:461–5.
17. Martinez IM, Velasquez P, Meseguer-Olmo L, Bernabeu-Esclapez A, de Aza PN. Preparation and characterization of novel bioactive α-tricalcium phosphate doped with dicalcium silicate ceramics. Mat Sci Eng C. 2012;32:878–86.
18. Elliot JC. Structure and chemistry of the apatites and other calcium orthophosphates. 3rd ed. Amsterdam: Elsevier Science BV; 1994.

19. Buerger MJ. Crystallographic aspects of phase transformations. In: Smoluchowski R, Meyer RJE, Weyl WA, editors. Phase transformations in solids. New York: Wiley; 1951. p. 183–211.
20. Carrodeguas RG, de Aza AH, Turrillas X, Pena P, de Aza S. New approach to the $\beta \rightarrow \alpha$ polymorphic transformation in magnesium-substituted tricalcium phosphate and its practical implications. J Am Ceram Soc. 2008;91(4):1281–6.
21. Nurse RW, Welch JH, Gutt W. High-temperature equilibria in the system dicalcium silicate-tricalcium phosphate. J Chem Soc. 1959;220:1077–83.
22. Fix W, Heymann H, Heinke R. Subsolidus relations in the system 2CaO·SiO2–3CaO·P2O5. J Am Ceram Soc. 1969;52(6):346–7.
23. Martinez IM, Velasquez P, De Aza PN. The system $Ca_3(PO_4)_2$–$Ca_2SiO_4$. The phase field tricalcium phosphate–silicocarnotite. J Am Ceram Soc. 2012;95(3):1112–7.
24. Eriksson G, Gu P, Blander M, Pelton AD. Critical evaluation and optimisation of the thermodynamic properties and phase diagrams of the MnO–$SiO_2$ and CaO–$SiO_2$ systems. Can Metall Q. 1994;33:13–21.
25. Mauney JR, Blumberg J, Pirun M, Volloch V, Vunjak-Novakovic G, Kaplan DL. Osteogenic differentiation of human bone marrow stromal cells on partially demineralized bone scaffolds "in vitro". Tissue Eng. 2004;10:81–92.
26. Scudiero DA, Shoemaker RH, Paull KD, Monks A, Tiemey S, Nofziger TH, et al. Evaluation of a soluble tetrazolium/formazan assay for cell growth and drug sensitivity in culture using human and other tumor cell lines. Cancer Res. 1988;48:827–33.
27. Kamitakahara M, Kurauchi T, Tanihara M, Ioku K, Ohtsuki C. Synthesis of Si-containing tricalcium phosphate and its sintering behaviour. Key Eng Mater. 2008;361–363:59–62.
28. Deans RJ, Moseley AB. Mesenchymal stem cells: biology and potential clinical uses. Exp Hematol. 2000;28(8):875–84.
29. Meseguer-Olmo L, Bernabeu-Esclapez A, Ros-Martinez E, Sanchez-Salcedo S, Padilla S, Martin AI, et al. "In vitro" behaviour of adult mesenchymal stem cells seeded on a bioactive glass ceramic in the SiO2–CaO–P2O5 system. Acta Biomater. 2008;4:1104–13.
30. Muller P, Bulnheim U, Diener A, Luthen F, Teller M, Klinkenberg ED, et al. Calcium phosphate surfaces promote osteogenic differentiation of mesenchymal stem cells. J Cell Mol Med. 2008;12:281–91.
31. Saldana L, Sanchez-Salcedo S, Izquierdo-Barba I, Bensiamar F, Munuera L, Vallet-Regi M, et al. Calcium phosphate-based particles influence osteogenic maturation of human mesenchymal stem cells. Acta Biomater. 2009;5:1294–305.
32. Martin JY, Schwartz Z, Hummert TW, Schraub DM, Simpson J, Lankford J, et al. Effect of titanium surface-roughness on proliferation, differentiation, and protein-synthesis of human osteoblast-like cells (MG63). J Biomed Mater Res. 1995;29:389–401.
33. Bowers KT, Keller JC, Randolph BA, Wick DG, Michaels CM. Optimization of surface micromorphology for enhanced osteoblast responses "in vitro". Int J Oral Maxillofac Implants. 1992;7: 302–10.
34. Boyan BD, Batzer R, Kieswetter K, Liu Y, Cochran DL, Szmuckler-Moncler S, et al. Titanium surface roughness alters responsiveness of MG63 osteoblast like cells to 1 alpha, 25-(OH)(2)D-3. J Biomed Mater Res. 1998;39:77–85.
35. Magallanes-Perdomo M, De Aza AH, Mateus AY, Teixeira S, Monteiro FJ, De Aza S, et al. "In vitro" study of the proliferation and growth of human bone marrow cells on apatite-wollastonite-2 M glass ceramics. Acta Biomater. 2010;6:2254–63.
36. Wu CT, Chang JA, Zhai WY, Ni SY, Wang JY. Porous akermanite scaffolds for bone tissue engineering: preparation, characterization, and "in vitro" studies. J Biomed Mater Res Part B. 2006; 78B(1):47–55.
37. ElGhannam A, Ducheyne P, Shapiro IM. Porous bioactive glass and hydroxyapatite ceramic affect bone cell function "in vitro" along different time lines. J Biomed Mater Res. 1997;36:167–80.
38. Elghannam A, Ducheyne P, Shapiro IM. Bioactive material template for in vitro synthesis of bone. J Biomed Mater Res. 1995;29:359–70.
39. Martinez IM, Meseguer-Olmo L, Bernabeu-Esclapez A, Velasquez P, De Aza PN. "In vitro" behavior of α-tricalcium phosphate doped with dicalcium silicate in the system $Ca_2SiO_4$–$Ca_3(PO_4)_2$. Mater Charact. 2012;63:47–55.
40. Ni SY, Chang J, Chou L, Zhai WY. Comparison of osteoblast-like cell responses to calcium silicate and tricalcium phosphate ceramics "in vitro". J Biomed Mater Res B Appl Biomater. 2007;80:174–83.
41. Sarmento C, Luklinska ZB, Brown L, Anseau M, De Aza PN, De Aza S, et al. "In vitro" behavior of osteoblastic cells cultured in the presence of pseudowollastonite ceramic. J Biomed Mater Res A. 2004;69A:351–8.
42. Gough JE, Jones JR, Hench LL. Nodule formation and mineralisation of human primary osteoblasts cultured on a porous bioactive glass scaffold. Biomaterials. 2004;25:2039–46.
43. Ming-You S, Shinn-Jyh D, Hsien-Chang Ch. The role of silicon in osteoblast-like cell proliferation and apoptosis. Acta Biomater. 2011;7:2604–14.
44. Tsigkou O, Jones JR, Polak JM, Stevens MM. Differentiation of fetal osteoblasts and formation of mineralized bone nodules by 45S5 Bioglass (R) conditioned medium in the absence of osteogenic supplements. Biomaterials. 2009;30:3542–50.
45. Botelho CM, Brooks RA, Kawai T, Ogata S, Ohtsuki C, Best SM, et al. In vitro analysis of protein adhesion to phase pure hydroxyapatite and silicon substituted hydroxyapatite. Key Eng Mater. 2005;284–286:461–4.
46. Gibson IR, Best SM, Bonfield W. Effect of silicon substitution on the sintering and microstructure of hydroxyapatite. J Am Ceram Soc. 2002;85:2771–7.
47. de Mate-Sanchez Val JE, Calvo-Guirado JL, Delgado-Ruiz RA, Ramirez-Fernandez MP, Martinez IM, Granero-Marin JM, Negri B, Chiva-Garcia F, Martinez-Gonzalez JM, de Aza PN. New block graft of α-TCP with silicon in critical size defects in rabbits: Chemical characterization, histological, histomorphometric and micro-CT study. Ceram Int. 2012;38:1563–70.
48. Xynos ID, Edgar AJ, Buttery LDK, Hench LL, Polak JM. Gene expression profiling of human osteoblasts following treatment with the ionic products of Bioglass ® 45S5 dissolution. J Biomed Mater Res. 2001;55:151–7.
49. Patel N, Best SM, Bonfield W, Gibson IR, Hing KA, Damien E, et al. A comparative study on the in vivo behavior of hydroxyapatite and silicon substituted hydroxyapatite granules. J Mater Sci Mater Med. 2002;13:1199–206.
50. Hench LL, Polak JM. Third generation biomedical materials. Science. 2002;295:1014–6.
51. Porter AE, Best SM, Bonfield W. Ultrastructural comparison of hydroxyapatite and silicon-substituted hydroxyapatite for biomedical applications. J Biomed Mater Res A. 2004;68:133–41.
52. Porter AE, Buckland T, Hing K, Best SM, Bonfield W. The structure of the bond between bone and porous silicon-substituted hydroxyapatite bioceramic implants. J Biomed Mater Res A. 2006;78:25–33.
53. Porter AE, Patel N, Skepper JN, Best SM, Bonfield W. Effect of sintered silicate substituted hydroxyapatite on remodelling processes at the bone–implant interface. Biomaterials. 2004;25:3303–14.
54. Curtis A, Wilkinson C. Topographical control of cells. Biomaterials. 1997;18:1573–83.